Molecular Crystals and Liquid Crystals Science and Technology. Section A. Molecular Crystals and Liquid Crystals

Publication details, including instructions for authors and subscription information:
http://www.tandfonline.com/loi/gmcl19

Theoretical Studies on Magnetic Interactions in Prussian Blue Analogs and Active Controls of Spin States by External Fields

Masamichi Nishino [a] , Shigehiro Kubo [a] , Yasunori Yoshioka [b] , Akira Nakamura [c] & Kizashi Yamaguchi [a]

[a] Department of Chemistry, Graduate School of Science, Osaka University, Toyonaka, Osaka, 560, Japan

[b] Takasago Laboratories, Kaneka Corporation, Miyamaemachi, Takasago-cho, Takasago, Hyogo, 676

[c] Department of Macromolecular Science, Graduate School of Science, Osaka University, Toyonaka, Osaka, 560, Japan

Version of record first published: 04 Oct 2006

To cite this article: Masamichi Nishino, Shigehiro Kubo, Yasunori Yoshioka, Akira Nakamura & Kizashi Yamaguchi (1997): Theoretical Studies on Magnetic Interactions in Prussian Blue Analogs and Active Controls of Spin States by External Fields, Molecular Crystals and Liquid Crystals Science and Technology. Section A. Molecular Crystals and Liquid Crystals, 305:1, 109-128

To link to this article: http://dx.doi.org/10.1080/10587259708045050

Mol. Cryst. Liq. Cryst., 1997, Vol. 305, pp. 109–128
Reprints available directly from the publisher
Photocopying permitted by license only

THEORETICAL STUDIES ON MAGNETIC INTERACTIONS IN PRUSSIAN BLUE ANALOGS AND ACTIVE CONTROLS OF SPIN STATES BY EXTERNAL FIELDS.

MASAMICHI NISHINO,[a] SHIGEHIRO KUBO,[a] YASUNORI YOSHIOKA[b] AKIRA NAKAMURA[c], AND KIZASHI YAMAGUCHI[a]

a) Department of Chemistry, Graduate School of Science, Osaka University, Toyonaka, Osaka 560, Japan

b) Takasago Laboratories, Kaneka Corporation, Miyamaemachi, Takasago-cho, Takasago, Hyogo 676.

c) Department of Macromolecular Science, Graduate School of Science, Osaka University, Toyonaka, Osaka 560, Japan

Abstract The symmetry rules for the d-orbital interactions are considered for simple prediction of the sign of effective exchange integrals between transition metal ions in Prussian blue analogs. Ab initio UHF and DFT calculations were carried out for binuclear transition-metal cyanides in order to elucidate variations of the through-bond exchange integrals with combinations of transition metal ions having different d-electron configurations. It was shown that the sign of effective exchange integrals predicted from the symmetry rules and the ab initio calculations are consistent with the experiments but their magnitudes calculated for tetracentric systems MCNM' (M=Cr(III), M'=V(II), Mn(II), etc.) by the use of triple zeta basis sets are larger than the observed values for Prussian blue analogs. The calculated results clearly indicated that the direct exchange interactions between M and M' are negligible, whereas the through-bond superexchange and spin polarization interactions are crucial for the high-T_c ferri (or ferro) magnetism in Prussian blue analogs. The modifications of electronic states in antiferromagnetic or paramagnetic precursors are also discussed in relation to our previous theoretical proposals for molecular spinics and recent experiments to obtain the switching type molecular magnets controlled by photochemical, electrochemical and other techniques.

INTRODUCTION

Theoretical studies on transition-metal complexes, clusters and solids have received continuous interest in relation to molecular design of functional materials. Over ten years ago, we attempted first principle calculations of the effective exchange integrals between transition metal ions via oxygen dianion. The antiferromagnetic exchange couplings for these species were well reproduced in our approximate spin projection

procedure for the unrestricted Hartree-Fock (UHF) solution in combination with the Heisenberg model.[1] It was found that the magnitude of the effective exchange integral (J_{ab}) for the copper oxide unit, Cu(II)-O-Cu(II), is abnormally large as compared with other transition metal oxides.[1] However, it was impossible to imagine that such a large $|J_{ab}|$ value may be closely related to the high-T_c superconductivity of copper oxides.[2] Therefore, after the discovery of the high-T_c superconductivity in the hole-doped states of these species, [3] we immediately carried out ab initio UHF calculations of several tricentric transition metal systems with and without holes.[4-6] From these calculations, a spin-fluctuation mechanism was proposed for the high-T_c superconductivity , and the T_c itself was also estimated from the calculated J_{ab} values.[4] We have also discussed possible electronic states generated from hole or electron doping into magnetic materials.[6] In the recent symposium [7,8] on the molecular magnetism, one of the authors (K. Y) emphasized that a next target in this field is an active control of magnetic states by thermal or photon modes such as the inter- and intra-molecular charge-transfer (CT) excitations.[9-12]

Past decade, many experiments have demonstrated that molecule-based magnets exhibit several spin-related phenomena such as spin alignment, spin gap, spin crossover, spin frustration and spin dynamics, some of which are now current topics in relation to new physics in the mesoscopic systems. [8] Active controls of these spin properties by chemical and physical techniques have been investigated extensively, [13] and a new filed, molecular "spinics" (spin+ics), is now developing rapidly. For example, from the viewpoint of the molecular spinics, Prussian blue type magnetic materials, $A_mM'_n[M(CN)_6]_l\ (H_2O)_y$, investigated by Girolami[14-16] , Verdaguer[17-19] and other[20,21] groups are particularly interesting because of several reasons: high transition temperature (T_c), varieties of transition metal combinations (M, M'), tunable magnetism, etc. Very recently, Hashimoto and Fujishima group[22-24] indeed reported the discovery of tunable magnetic phase transition of chromium cyanide thin film controlled by the electrochemical method. Their group also found the photo-induced magnetic phase transitions in Prussian blue analogs. Thus active controls of electronic and magnetic properties of Prussian blue analogs are now current topics.[14-24]

Here, as a continuation of previous work,[4-12] the symmetry rules[25,26] for the d-orbital interactions are considered for simple prediction of the sign of the effective exchange integrals between transition metal ions in the octahedral ligand field since Prussian blue analogs[14-24] have the face-centered-cubic lattices. The ab initio UHF and DFT calculations of bicentric systems, MM', tetracentric systems, MCNM', and octacentric systems, NCMCNM'NC (M=Cr(III), M'=Cr(III), Cr(II), Ni(II) and Mn(II)

), are performed in order to elucidate the sign and magnitude of J_{ab} values of these systems. [1,27,28] These calculated results are analyzed to obtain theoretical explanations of the possible mechanisms of the direct exchange interaction between M and M', and their indirect interaction via the cyano group. Implications of the calculated results are discussed in relation to possible modifications of antiferro- or para-magnets into ferro- or ferri-magnetic systems by electron or hole doping and CT excitations.[6-12]

ORBITAL SYMMETRY RULES FOR MCNM' SYSTEMS

(A) Direct Exchange Interactions

First, let us consider the symmetry rules for the d-d orbital interactions to elucidate the direct interactions between transition metal ions. To this end, Table I summarizes the electronic configurations of transition metal ions and possible spin states in the octahedral ligand field. Figure 1 illustrates the direct and indirect orbital interactions between the d-orbitals. The contributions of the CN group are neglected in the direct interaction. Since there are several open-shell orbitals on each site, the effective exchange integral between transition metal ions is given by the sum of all the effective orbital exchange integrals as

$$J_{MM'} = \sum_{i=1}^{m}\sum_{j=1}^{n} J_{ij} \qquad (1)$$

where m and n denote, respectively, the numbers of the open-shell orbitals on the transition-metal ions M and M'. According to the orbital symmetry rules for the d-d direct interactions, the nonzero orbital-overlap (OO) integral between the t_{2g} (or e_g) orbitals should provide the antiferromagnetic kinetic exchange (KE) interaction; J_{ij}(KE) <0. While the zero-overlap integral between the orthogonal t_{2g} and e_g orbitals gives rise to the ferromagnetic exchange interaction via the Coulombic potential; J_{ij} (PE)>0. However, judging from the previous computational results, [27] these direct exchange interactions might be negligibly small because of the long M-M' distances in Prussian blue analogs.

(B) Superexchange interactions.

Next, the indirect (through-bond) interactions between transition metal ions via ligands X-Y were examined.[27] Figure 1 illustrates possible superexchange (SE) paths [25,26] via the molecular orbitals (MO) of the coupler groups X-Y, where X-Y= $C\text{-}C^{2-}$, CN^{1-}, N=N, NO^{1+} etc. These isoelectronic ligands have the following MOs: X-lone pair, X-Y σ-bond, Y-lone pair, two π-orbitals and two π^*-orbitals. Therefore there

TABLE I Electronic configurations and possible spin states of transition metal ions

No.	Configurations	Spin States *	Examples
1	$(t_{2g})^1$	(S=1/2)	Ti^{3+}, V^{4+}, Cr^{5+}, Mn^{6+}
2	$(t_{2g})^2$	(HS, S=2/2), (LS, S=0),	Ti^{2+}, V^{3+}, Cr^{4+}, Mn^{5+}
3	$(t_{2g})^3$	(HS, S=3/2), (LS, S=1/2)	V^{2+}, Cr^{3+}, Mn^{4+}
4	$(t_{2g})^4$	(IS, S=2/2), (LS, S=0)	V^{1+}, Cr^{2+}, Mn^{3+}, Fe^{4+}
5	$(t_{2g})^3(e_g)^1$	(HS, S=4/2)	"
6	$(t_{2g})^5$	(LS, S=1/2)	Mn^{2+}, Fe^{3+}, Co^{4+}
7	$(t_{2g})^4(e_g)^1$	(IS, S=3/2)	"
8	$(t_{2g})^3(e_g)^2$	(HS, S=5/2)	"
9	$(t_{2g})^6$	(LS, S=0)	Fe^{2+}, Co^{3+}, Ni^{4+}
10	$(t_{2g})^5(e_g)^1$	(IS, S=2/2)	"
11	$(t_{2g})^4(e_g)^2$	(HS, S=4/2)	"
12	$(t_{2g})^6(e_g)^1$	(LS, S=1/2)	Co^{2+}, Ni^{3+}
13	$(t_{2g})^5(e_g)^2$	(HS, S=3/2)	"
14	$(t_{2g})^6(e_g)^2$	(HS, S=2/2), (LS, S=0)	Ni^{2+}, Cu^{3+}
15	$(t_{2g})^6(e_g)^3$	(S=1/2)	Ni^{1+}, Cu^{2+}

*HS: High-spin state, IS: Intermediate spin state and LS: Low-spin state.

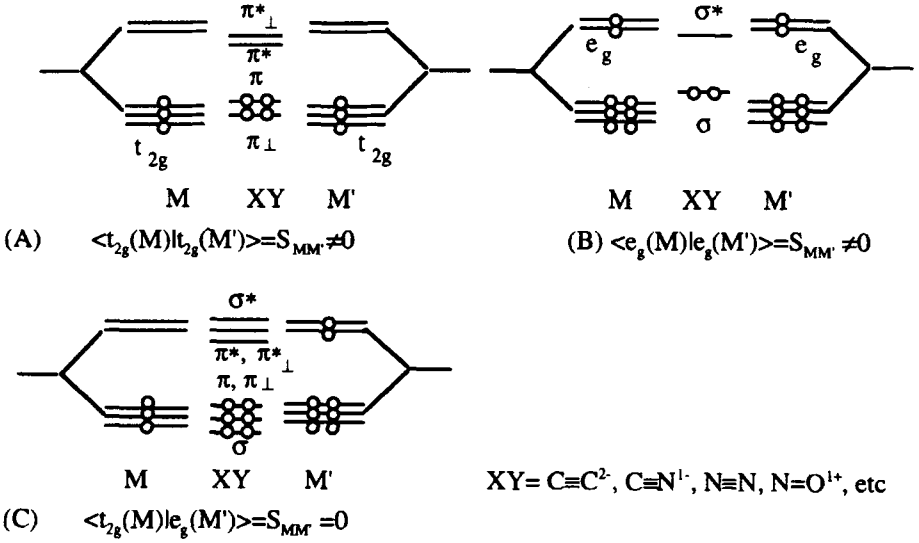

FIGURE 1 Possible direct and super-exchange interaction paths for the MXYM' system. A and B denote, respectively, the antiferromagnetic exchange interactions between t_{2g} orbitals and between e_g orbitals. On the other hand, C denotes the ferromagnetic interaction between t_{2g} and e_g orbitals.

are three different through-bond interactions: one is the through σ-bond interaction, through π- and through orthogonal π-orbital interactions. Figure 2 illustrates the superexchange interactions through these orbitals. The CT from the occupied π-MO of X-Y to the d-orbital of M generates the unpaired electron in the π-MO, which interacts with the unpaired d-electron of M'. If the orbital overlap between the open-shell π- and d-orbitals is not zero, this orbital-overlap (OO) term leads to the nonzero stabilization of the singlet state, namely J_{ij} (SE) <0. On the other hand, if these radical orbitals are orthogonal, the potential exchange term becomes predominant in the CT configuration, leading to the ferromagnetic superexchange interaction; J_{ij} (SE)>0. Therefore, the net results arising from the superexchange (SE) interactions are quite similar to those of the direct exchange interactions.

The possible spin alignments are easily predicted from the following assumptions.

Rule1: The antiparallel spin alignment is expected if one of the possible orbital superexchange integrals J_{ij} is negative (antiferromagnetic), though several orbital ferromagnetic terms are operative in Equation (1).

Rule2: The parallel spin alignment is expected if all of the possible orbital superexchange integrals are positive (ferromagnetic) in Equation (1).

Table II summarizes possible spin alignments derived from these spin alignment rules based on the orbital interaction schemes in Figure 2.

From Table II, the antiferromagnetism is expected for the transition metal pair with zero net spin moment. On the other hand, the ferrimagnetism is

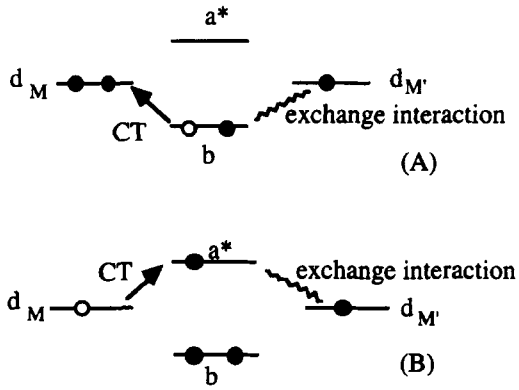

FIGURE 2 The superexchange interaction schemes via the CT configurations (A) b-path and (B) a*-path. The sign of the superexchange integrals is determined by the orbital overlap integral between the singly occupied orbitals.

TABLE II Spin alignment rules based on the superexchange mechanism.

	1	2(HS)	3(HS)	3(LS)	5	6	7	8	10	11	12	13	14(HS)	15	X[a]
1	AF	FI	FI	AF	FI	AF	FI	FI	FI	FI	F	FI	F	F	P
2(HS)		AF	FI	FI	FI	FI	FI	FI	AF	FI	F	FI	F	F	P
3(HS)			AF	FI	FI	FI	AF	FI	FI	FI	F	FI	F	F	P
3(LS)				AF	FI	AF	FI	FI	FI	FI	F	FI	F	F	P
5					AF	FI	FI	FI	FI	AF	FI	FI	FI	FI	P
6						AF	FI	FI	FI	FI	F	FI	F	F	P
7							AF	FI	FI	FI	FI	FI	FI	FI	P
8								AF	FI	FI	FI	FI	FI	FI	P
10									AF	FI	FI	FI	AF	FI	P
11										AF	FI	FI	FI	FI	P
12											AF	FI	FI	AF	P
13												AF	FI	FI	P
14(HS)													AF	FI	P
15														AF	P
X															D

a) X=2(LS), 4(LS), 9, 14(LS), b) AF=antiferromagnetic, FI=ferrimagnetic, F=ferromagnetic, P=paramagnetic and D=diamagnetic

predicted for the antiparallel spins with different sizes. Therefore there are many combinations of transition metal ions, which in principle provide the ferrimagnetism. On the other hand, there are several ferromagnetic pairs such as Cr(III)-Ni(II) and Cr(III)-Cu(II) as shown in Table II since their magnetic orbitals are orthogonal.

(C) The Double Exchange and Spin Polarization Effects

The double exchange mechanism may become important if the occupied d-orbital level becomes close to that of the partner ion. The potential exchange interaction within the metal ion favors the high spin state as illustrated in Figure 3. Therefore, many ferrimagnetic states are converted into the ferromagnetic states if the double exchange mechanism[29,30] is more significant than the superexchange mechanism.

Both the σ- and π-type spin polarization mechanisms are also conceivable in the M-X-Y-M' systems. The spin alternation on the π-electron system leads to the antiferromagnetic spin alignment as illustrated in Figure 4A. Similarly the spin polarization via the σ-electron also gives rise to the antiparallel spin alignment as

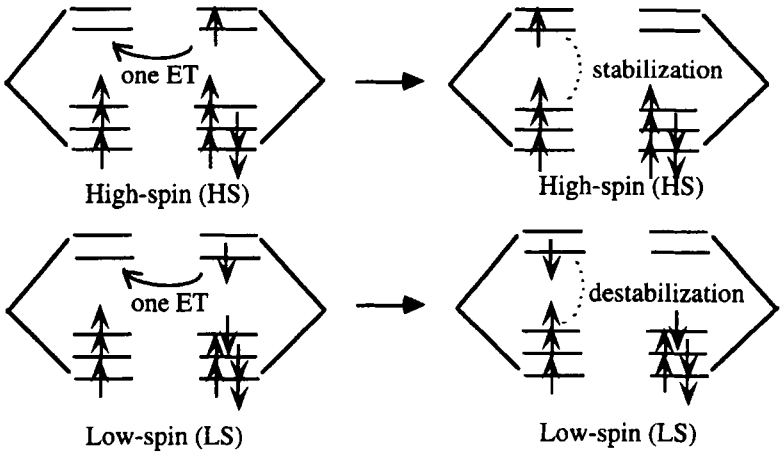

FIGURE 3 Stabilization of the high-spin (HS) state and destabilization of the low-spin (LS) state by the double exchange mechanism.

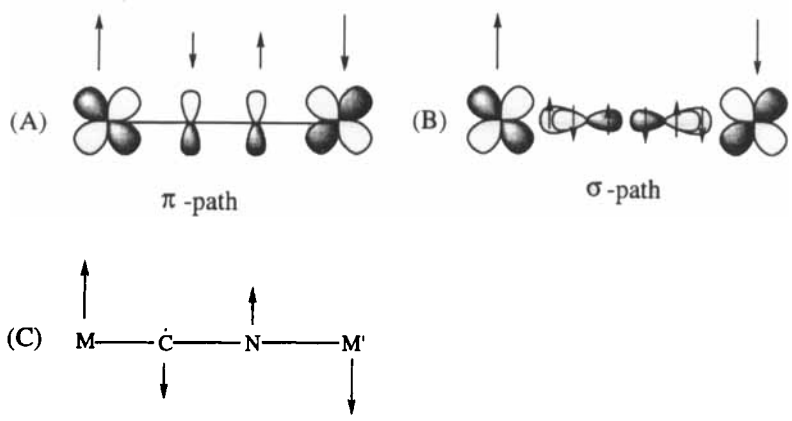

FIGURE 4 Schematic illustrations of the spin polarization (SP) effects. A, B and C denote, respectively, the π- and σ-type SP paths, and the spin structure.

illustrated in Figure 4B. From Figure 4C, the negative spin density should appear on the carbon atom as confirmed by the later ab initio calculations.

ELECTRONIC STRUCTURES AND SPIN STATES OF PRUSSIAN BLUE ANALOGS

(A) Qualitative Theoretical Explanations of Magnetic Interactions

Recently there are many experimental reports for Prussian blue analogs.[14-24] Table III summarizes the combinations of transition metal ions reported in these papers. The electronic configurations of the component transition metal ions are also summarized in Table III. According to the spin alignment rules in Table II, the plausible magnetic orderings can be easily predicted. For example, the effective exchange interaction between Cr(III) and V(II) (or V(III)) should be antiferromagnetic. On the other hand, the interaction between Cr(III) and Ni(II) (or Cu(II)) is predicted to be ferromagnetic because of the orthogonality between the t_{2g} and e_g-orbitals. The theoretical results are wholly compatible with the experimental results available[14-24] as shown in Table III.

(B) Ab initio Calculations

The molecular orbital (MO) calculations were carried out to confirm the preceding qualitative results. Figure 5A shows the orbital interaction diagram in the M-M' systems at the Extended Hückel MO level. The symmetric (S) and antisymmetric (A)

TABLE III The d-electron configurations of transition metal ions (M, M') and the magnetic couplings between M and M'.

System	M	M'	Magnetic Couplings	Exp.***
1	Cr(III): $(t_{2g})^3$(S=3/2)	Cr(II): $(t_{2g})^3(e_g)^1$(S=4/2)	Ferri	Ferri[17, 22]
2	Cr(III): $(t_{2g})^3$(S=3/2)	Cr(III): $(t_{2g})^3$ (S=3/2)	Antiferro	Antiferro[17, 22]
3	Cr(III): $(t_{2g})^3$(S=3/2)	V(II): $(t_{2g})^3$ (S=3/2)	Antiferro	Antiferro[18]
4	Cr(III): $(t_{2g})^3$ (S=3/2)	V(III): $(t_{2g})^2$ (S=2/2)	Ferri	Ferri[18]
5	Cr(III): $(t_{2g})^3$ (S=3/2)	Ni(II): $(t_{2g})^6(e_g)^2$(S=2/2)	Ferro	Ferro[19]
6	Mn(II): $(t_{2g})^3(e_g)^2$(S=5/2)	Mn(II): $(t_{2g})^5$ (S=1/2)	Ferri	Ferri[14]
7	Mn(II): $(t_{2g})^3(e_g)^2$(S=5/2)	Mn(III): $(t_{2g})^4$ (S=2/2)	Ferri	Ferri[14]
8	Mn(II): $(t_{2g})^3(e_g)^2$(S=5/2)	Mn(IV): $(t_{2g})^3$ (S=3/2)	Ferri	Ferri[20]
9	Mn(II): $(t_{2g})^3(e_g)^2$(S=5/2)	V(II): $(t_{2g})^3$ (S=3/2)	Ferri	Ferri[15]
10	Mn(II): $(t_{2g})^3(e_g)^2$(S=5/2)	Cr(III): $(t_{2g})^3$ (S=3/2)	Ferri	Ferri[16]
11	Mn(III): $(t_{2g})^4$ (S=2/2)	Ni(II): $(t_{2g})^6(e_g)^2$(S=2/2)	Ferro	Ferro[16]
12	Fe(III): $(t_{2g})^5$(S=1/2)	Co(II): $(t_{2g})^5(e_g)^2$(S=3/2)	Ferri*	
			Ferro**	Ferro[23]
13	Fe(III): $(t_{2g})^5$(S=1/2)	Ni(II): $(t_{2g})^6(e_g)^2$(S=2/2)	Ferro	Ferro[21]
14	Fe(III): $(t_{2g})^5$(S=5/2)	Cu(II): $(t_{2g})^6(e_g)^3$(S=1/2)	Ferri	Ferri[21]

*: superexchange mechanism; **: double exchange mechanism; *** references

molecular orbitals (ϕ_S, ϕ_A) are formed from the symmetry requirement. However, because of the near degeneracy between the S and A MOs, the magnetic orbitals based on the UHF and DFT approximations[1,27] are given by

$$\phi_a \text{ (up spin)} = \cos\theta\ \phi_S + \sin\theta\ \phi_A \quad (2a)$$

$$\phi_b \text{ (down spin)} = \cos\theta\ \phi_S - \sin\theta\ \phi_A . \quad (2b)$$

From Figure 5A, the magnetic orbitals are symmetry-broken and are essentially localized on the left and right transition metal ions, respectively, if the interatomic distance exceeds a certain limit.

The above localized magnetic orbitals interact with the bonding (b) σ or π- and antibonding (a*) σ*- or π* -MOs of the coupler group as illustrated in Figure 5B. The mixing ratio between the d- and π(or π*) MOs is dependent on their energy gaps and magnitude of the interaction matrix elements (see below). The magnetic orbitals for the up- and down-spins via the superexchange mechanisms are generally given by

$$\psi_M \text{ (up spin)} = N_M \{ \phi_a + C_1\pi + C_2\pi^* \} \quad (3a)$$

$$\psi_{M'} \text{ (down spin)} = N_{M'} \{ \phi_b + C_3\pi + C_4\pi^* \} \quad (3b)$$

where N_M and $N_{M'}$ are the normalizing factors, and C_1-C_4 denote the orbital mixing

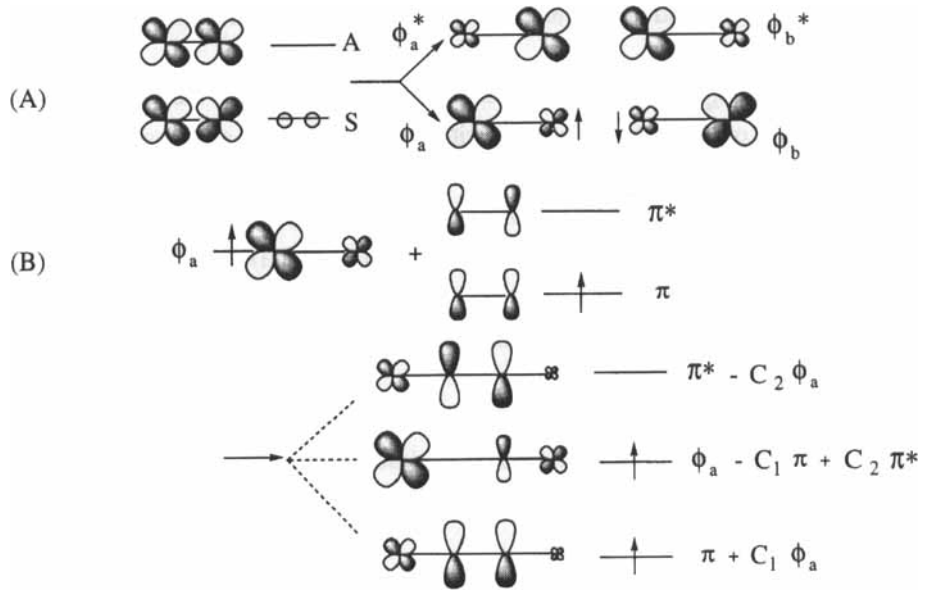

FIGURE 5 The orbital interactions between d- and π (or π*) MOs. A and B denote, respectively, the direct and indirect orbital interactions between transition-metal ions.

coefficients determined by the UHF and DFT calculations.[21]

As an example, Figures 6A and B show the magnetic t_{2g} orbitals calculated for the M-CN-M' systems (M=Cr(III), V(II), M'=Cr(III), V(II), Mn(II)) by the UHF and DFT methods. The following triple-zeta (TZ) basis sets were used: the Tatewaki-Hujinaga MIDI[31] plus Hay's diffuse d-basis sets: (533(21)/53(21)/411 for transition metal ions and 6-31G plus diffuse sp-and d-polarization orbitals for C and N . Figure 6C shows the magnetic t_{2g} orbitals of Cr(III) and magnetic e_g orbitals of Ni(II) in the Cr(III)-CN-Ni(II) system obtained by the UHF/TZ calculation. For comparative purpose, the e_g orbitals of Mn(II) obtained for Cr(II)-CN-Mn(II) by both the UHF and DFT/TZ methods are also shown in Figure 6D.

From Figure 6, the following conclusions are drawn:

(1) The magnetic t_{2g} orbitals of Cr(III) and Mn(II) by the ab initio UHF method are essentially localized on each atomic site, whereas that of V(II) is significantly delocalized over the CN group.

(2) The magnetic t_{2g} orbital of Cr(III) by the DFT (B2LYP) method is a little delocalized over the CN group, but that of Mn(II) is significantly delocalized over the CN group in the case of V(II)-CN-Mn(II). The magnetic t_{2g} orbitals of Mn(II) and V(II) are delocalized even over the Cr(III) ion in the cases of Cr(III)-CN-Mn(II) and Cr(III)-CN-V(II).

(3) The magnetic t_{2g} orbitals of Cr(III) are essentially localized on the atomic site, while the e_g orbital of Ni(II) interacts with the σ^* MO of CN, showing the significant delocalization in the Cr(III)-CN-Ni(II) system. The orthogonality between these t_{2g} and e_g orbitals is clear as required for the ferromagnetic interaction.

(4) The e_g orbital of Mn(II) obtained for the Cr(III)-CN-Mn(II) system by DFT is delocalized over the partner Cr(III) ion, showing an important contribution of the double exchange interaction. On the other hand, such an interaction becomes weak under the UHF approximation.

From these conclusions, the orbital interaction schemes are different between UHF and DFT in several cases. The DFT method is biased to provide delocalized d-orbitals; namely the covalent bonding character is remarkable.

(C) Calculations of $J_{MM'}$ values by ab initio UHF and DFT

Although the magnetic orbitals are more or less delocalized over the CN group, they are largely symmetry-broken at the magnetic centers. Therefore, the Heisenberg model is formally used to describe the energy gaps between the high-spin (HS) and

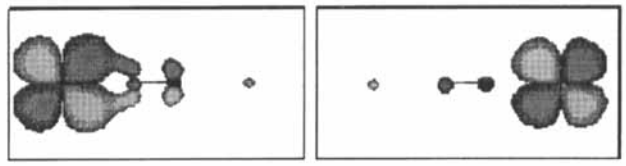

Cr(III)-CN-Cr(III)

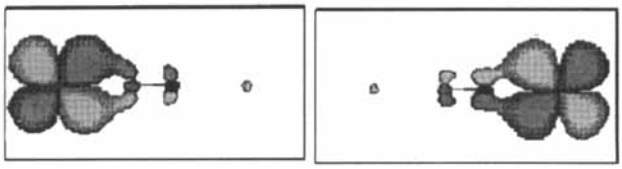

Cr(III)-CN-Mn(II)

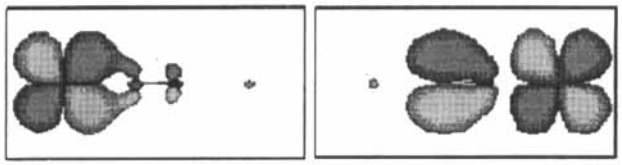

Cr(III)-CN-V(II)

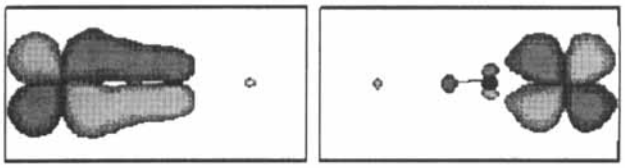

V(II)-CN-Mn(II)

(A)

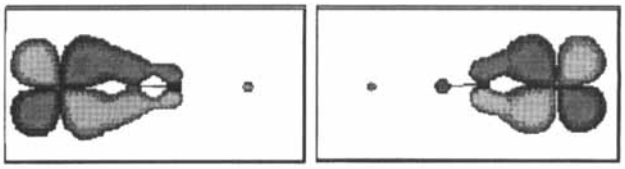

Cr(III)-CN-Cr(III)

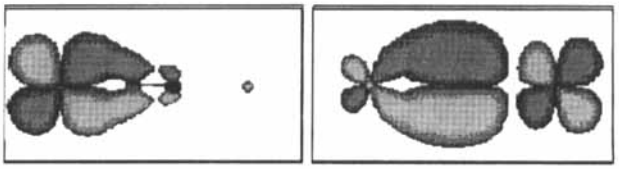

Cr(III)-CN-Mn(II)

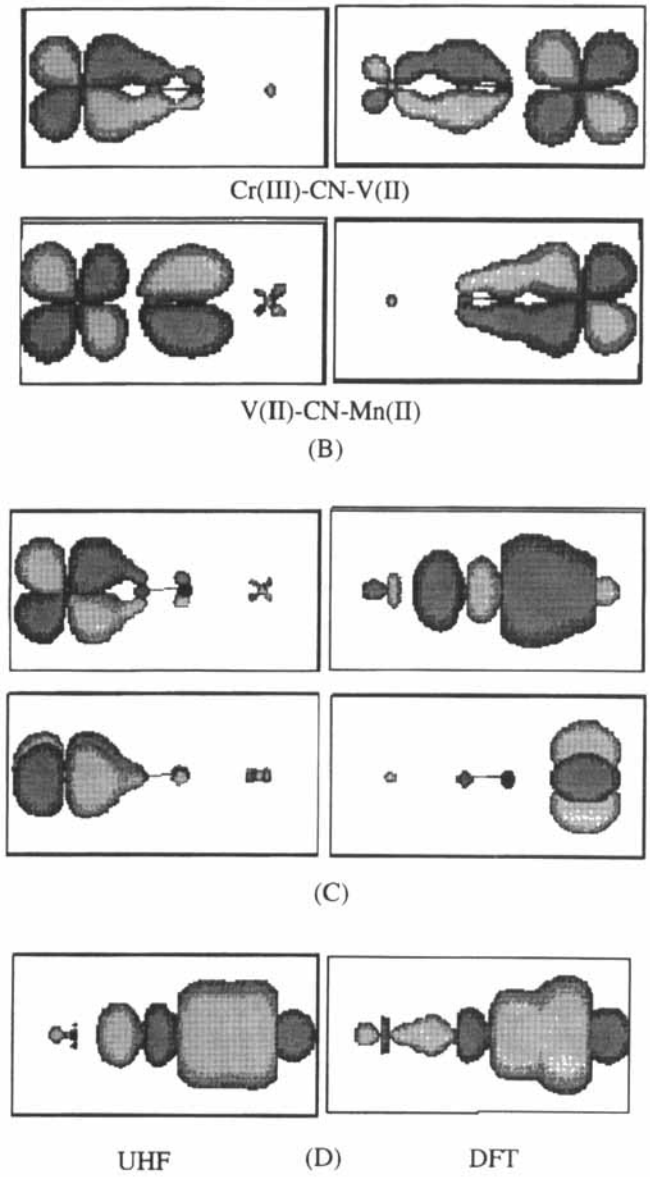

FIGURE 6 The t_{2g} orbitals for the up- and down-spins in the M-CN-M' systems by the UHF (A) and DFT(B) calculations. The orthogonal t_{2g} and e_g orbitals for the Cr(III)-CN-Ni(II) system are shown in C, whereas the e_g orbitals for Mn(II) of the Cr(III)-CN-Mn(II) by the UHF and DFT methods are given in D.

low-spin (LS) states. The effective exchange integrals ($J_{MM'}$) were easily calculated by the combination of the UHF or DFT method with the Heisenberg model (HB)[1,27] as

$$J_{AP-X} = \frac{^{HS}E_X - ^{LS}E_X}{^{HS}\langle S^2 \rangle_X - ^{LS}\langle S^2 \rangle_X} (X = UHF, DFT) \qquad (4)$$

where $^{Y}E_X$ and $^{Y}\langle S^2 \rangle_X$ denote, respectively, the total energy and total angular momentum for the spin state Y by the method X.

Table IV summaizes the $J_{MM'}$ values calculated for MM', MCNM' and NCMCNM'NC by the AP-UHF and AP-DFT methods. The geometries for these model systems were taken from the experiments. [14-24] From Table IV, the following conclusions were obtained:

(1) The direct exchange interactions between the transition metal ions are almost zero because their interatomic distances are over 5 Å in the Prussian blue analogs.

(2) The signs of the $J_{MM'}$ values calculated for MCNM' by the APUHF method are consistent with those predicted from the symmetry rules, and the experiments available.[14-24] This indicates that the through-bond exchange interaction plays a crucial role in Prussian blue analogs.

TABLE IV The effective exchange integrals between the transition metal ions (M, M') in Prussian blue analogs.

System	$J_{MM'}$(UHF)	$J_{MM'}$(DFT)	$J_{MM'}$(exp.)
Cr(III)Cr(III)	0.000	0.000	
Cr(III)Mn(II)	0.000		
Cr(III)V(II)	0.000		
Cr(III)NI(II)	0.001		
V(II)Mn(II)	0.011	-0.002	
Cr(III)CNCr(III)	-232.7		
Cr(III)CNMn(II)	-25.4	24.5	
Cr(III)CNV(II)	-143.9	-104.8	
Cr(III)CNNi(II)	63.7	49.9	
Cr(III)CNV(III)	-173.0	-35.0	
V(II)CNMn(II)	-11.5	-11.4	
NCCr(III)CNMn(II)NC	-48.2		-4
NCCr(III)CNNi(II)NC	40.2		8.5

(3) The magnitudes of the $J_{MM'}$ values calculated for MCNM' are much larger than the experimental values determined for the real Prussian blue analogs. The situation is similar even for the NCMCNM'NC systems.

(4) The $J_{MM'}$ value for the Cr(III)-CN-Mn(II) by the DFT method becomes positive in sign because of the double exchange mechanism. This is consistent with the e_g orbital delocalization of Mn(II) in Figure 6D.

From these conclusions, it is clear that the ab initio calculations predict reasonable tendencies in the exchange interactions between M and M' but the magnitude of the calculated $J_{MM'}$ values are sensitive to environmental effects such as the number of CN group. Therefore ab initio calculations of more larger clusters are necessary for further discussions.

(D) Calculations of the Spin Densities

The ab initio UHF and DFT calculations clearly indicated that the negative spin densities appear on the carbon atom. This indicates that the spin polarization (SP) effect plays an important role for the through-bond interaction between the transition-metal ions. Table V summarizes the atomic spin densities calculated for the MCNM' and NCMCNM'NC systems by the DFT method. The spin density on the Cr(III) atom in the model systems becomes larger than 3.0, whereas the spin density on the carbon atom becomes smaller than -0.2. Apparently, the SP mechanism acts effectively on

TABLE V The atomic spin densities calculated for the M-C-N-M' systems by the DFT (U-B2LYP)/TZ method.

System	2S+1	M	C	N	M'
Cr(III)-CN-Cr(III)	1	3.25	-0.52	0.46	-3.19
Cr(III)-CN-Mn(II)	3	3.35	-0.61	0.26	-5.00
	9	3.42	-0.44	0.09	4.93
Cr(III)-CN-V(II)	1	3.31	-0.66	0.28	-2.93
	7	3.37	-0.49	0.15	2.97
Cr(III)-CN-Ni(II)	2	3.34	-0.54	0.19	-1.99
	6	3.36	-0.56	0.25	1.95
Cr(III)-CN-V(III)	2	3.25	-0.45	0.28	-2.08
	6	3.24	-0.40	0.06	2.10
V(II)-CN-Mn(II)	3	2.99	-0.22	0.22	-4.99
	9	2.99	-0.07	0.09	4.99

the MCNM' network, giving rise to the antiferromagnetic contribution; M(↑)-C(↓)-N(↑)-M'(↓) as illustrated in Figure 4C. The decomposition of atomic spin density into the σ- and π- contributions indicates that the SP effect via the π–network is more significant than the σ–contribution. Probably, this is a characteristic of the d-π-conjugated systems.

ACTIVE CONTROLS OF MAGNETISM BY EXTERNAL VARIABLES

(A) Hubbard Models for Prussian Blue Analogs

The computational results in Figure 6 show that the orbital interactions are sensitive to the computational procedures. It is noteworthy that the ab initio UHF method is biased to the localized description, whereas the DFT method favors the delocalized description. Apparently more refined methods are necessary for the first principle calculations of the d-p covalent bondings. This in turn indicates the semiempirical models are still useful for molecular design of Prussian blue analogs having desired properties. Here, Hubbard models[32] are considered in order to clarify the key factors controlling the electronic structures of Prussian blue analogs. Generally speaking, electronic, magnetic, optical and other properties of these species are governed by three important microscopic variables: (1) transfer integral (T), (2) electron-phonon (lattice) interaction (W) and electron-electron interaction (U).[8] T describes the itinerant character of electron or hole. Figure 7 illustrates three T-parameters for MCNM' : T_1 denotes the transfer integral between M and C, and T_2 denotes that between N and M'. The transfer integral T_3 between C and N is considered to be constant but the electron phonon (lattice) coupling W via the CN group is considered to be an important parameter The on-site repulsion term U is explicitly considered for the transition metal ions: U_M and $U_{M'}$. The orbital energies $\varepsilon_{M(M')}$ and the repulsion terms $U_{M(M')}$ are given in previous papers. [33] Therefore, any property (P) of Prussian blue analogs can be described by these variables: P = functions (T, W, U,) and the extended Peirles Hubbard Hamiltonian involving these parameters should have a general applicability to theoretical treatments of the species. However, several characteristic cases are approximately described by depicting the orbital energy diagrams as shown in Figure 8.

(a) Localized limit ; The d-orbital levels are far different from the π– and π* MO levels. The d-electrons are essentially localized on the transition metal ions because of the small d-π(π*) mixing. The perturbation theory can be applicable to the estimation of the contribution of the superexchange interaction in Figure 5,

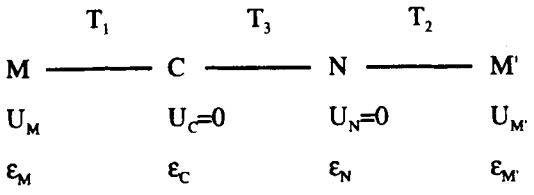

FIGURE 7 The parameters in the Hubbard model for the M-CN-M' system. The notations T, U and ε are given in the text.

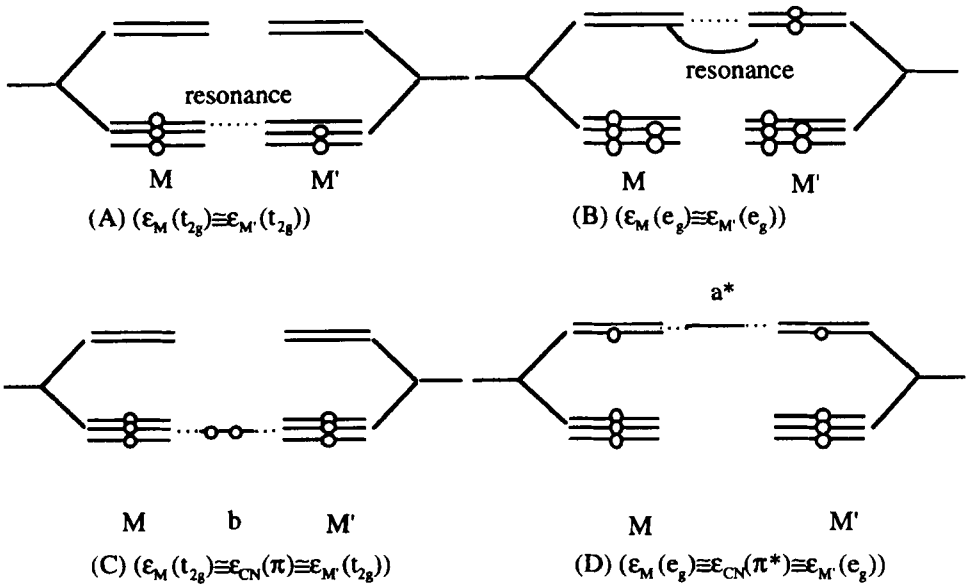

FIGURE 8 The orbital interaction diagrams responsible for the d-orbital resonances on the basis of the Hubbard models. A and B denote, respectively, the double resonance and triple resonance cases.

and the d-π(π*) mixing coefficients are approximately given by

$$C_{1(3)} = T_{1(2)} / (\varepsilon_{M(M')} - \varepsilon_{\pi} + U_{M(M')}) \quad (5a)$$

$$C_{2(4)} = T_{1(2)} / (\varepsilon_{\pi^*} - \varepsilon_{M(M')}). \quad (5b)$$

For example, the d-π mixing in the Cr(III)-CN-Mn(II) system is very small under the UHF approximation as shown in Figure 6A. This corresponds to a localized limt described by Equation (5).

(b) Half-delocalized case; One of the d-orbital levels is close to that of the π (or π*) .

Therefore the half and half mixing occurs between these two levels. For example,

$$\psi_M = N_M \{\phi_a + \pi (\pi^*)\} \quad \text{or} \quad \psi_{M'} = N_{M'} \{\phi_b + \pi (\pi^*)\} \tag{6a}$$

where $\varepsilon_M = \varepsilon_{\pi(\pi^*)}$ or $\varepsilon_{M'} = \varepsilon_{\pi(\pi^*)}$ (6b)

The t_{2g} orbitals for V(II) in the Cr(III)-CN-V(II) and V(II)-CN-Mn(II) systems by the UHF method are delocalized over the CN group, showing the strong d-π interaction (see Figure 6A).

(c) Delocalized cases; There are two delocalized limits. One is the resonance state of the degenerate d-orbitals; one electron transfer (ET) is therefore feasible between them. One ET is responsible for the double exchange mechanism in Figure 3

$$\psi_{M(M')} = \phi_S \text{ or } \phi_A . \tag{7}$$

The other is the resonance state of the three orbitals; d-$\pi(\pi^*)$-d;

$$\psi_{M(M')} = N_{M(M')} \{\phi_a + \pi (\pi^*) + \phi_b\}. \tag{8}$$

For example, the DFT t_{2g} orbitals for V(II) in the Cr(III)-CN-V(II) system and for Mn(II) in the Cr(III)-CN-Mn(II) system delocalize over the Cr(III) ion because of the near degeneracy though such delocalizations do not occur under the UHF approximation. This indicates that the d-orbital level is different between the UHF and DFT methods. The Hubbard models based on the above classification will be used for future semiempirical explanation of the experiments.[14-24]

(B) Active Controls of Spin states of Prussian Blue Analogs

Previously[6-12,27,28], we have emphasized that active controls of spin states by external fields are important for potential applications of molecule-based materials to advanced technologies. Concerning with these applications, there are several reasons why Prussian blue analogs are so interesting:[14-24]

(1) The effective exchange interactions between M and M' via CN anion are strong.

(2) The solids are easily prepared from cyanometallate building blocks.

(3) The oxidation or reduction states of transition metal ions are often sensitive to external variables (concentration of alkali metals, electron donors, external electronic field, photoexcitation, etc).

(4) Controls of spin properties with the above variables are feasible in appropriate experimental conditions.

In fact, Girolami and Verdaguer groups have discussed that switchings of electronic, magnetic and optical properties by the external fields are key issues for Prussian blue analogs[14-21]. Hashimoto and Fujishima group[22-24] have first demonstrated the tunable molecular magnetisms in these systems.

(C) Theoretical Possibilities of Molecular Spinics in Prussian Blue Analogs

There are many theoretical possibilities to modify the electronic and spin states of Prussian blue analogs. From Tables II-V and Figures 1-7, the following modification procedures are conceivable.

(1) d-level controls: The through-bond exchange interactions between transition-metal ions are sensitive to the d-orbital energy levels which are controllable with selecting alkali metal cations and other donor cations (see Figure 8). The transition temperatures should be raised by these substitutions.

(2) doping (oxidation or reduction): The electron or hole doping (reduction or oxidation) into transition-metal ions or linkage groups by several techniques may induce the magnetic phase transitions: for example, antiferromagnetis state ↔ ferri- or ferro-magnetic state.

(3) CT excitation: The charge transfer excitations between transition-metal ions induced by thermal and photochemical techniques may induce the magnetic phase transitions: for example, antiferromagnetic (or diamagnetic) state ↔ ferri- or ferro-magnetic state.

(4) substitutions of transition-metal ions: The partial substitutions of transition metal ions for other transition-metal ions may induce variations of the magnetic states in Prussian blue analogs.

(5) substitutions of linkage groups: The partial substitutions of cyano groups with other linkage groups may induce variations of the magnetic states in Prussian blue analogs (see Figure 1).

Figure 9 illustrates possible magnetic phase transitions induced by the above techniques. Probably many experimental efforts for active controls of the magnetic states in Prussian blue analogs will appear in the next few years.

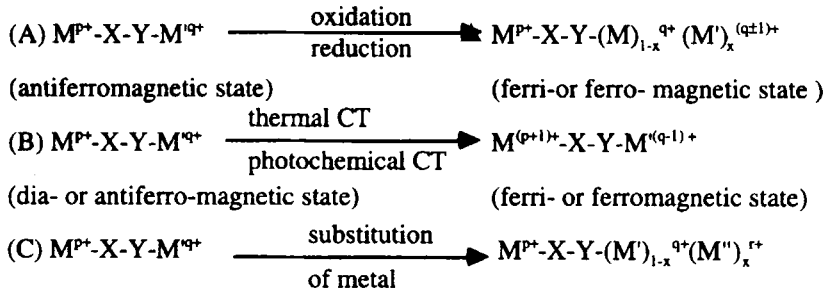

FIGURE 9 Active controls of the magnetic states in Prussian blue analogs by the doping (A), thermal and photochemical charge-transfer (CT) (B) and substitutions of transition-metal ions (C).

CONCLUSIONS

Recent experiments[14-24] clearly demonstrated that dynamic controls of the magnetic phases in Prussian blue analogs are feasible by several techniques such as hole or electron doping[4-6] and charge transfer (CT) excitation[7-12]. These experimental results support our previous theoretical proposals[4-6] for modifications of molecule-based magnets into functional materials. From the same guiding principles [7-12], pure organic CT complexes with spins are also interesting targets for the dynamic controls of magnetic phases. For example, the high-T_c organic CT ferrimagnets, ferri(or ferro) magnetic metals,[34] and spin-mediated organic superconductors remain as theoretical proposals[6-12], but they will be discovered near future. In fact, several preliminary experiments[35] have been carried out for syntheses of these new materials. In conclusion, a new field, molecular spinics, is developing rapidly under the interplay between theories and experiments.

ACKNOWLEDGMENT

One of the authors (K. Y) thanks Professor M. Verdaguer and Professor K. Hashimoto for helpful discussions on the molecular spinics in Prussian blue analogs. The authors gratefully acknowledge the financial support of the Ministry of Education, Science and Culture of Japan (Specially Promoted Research No.06101004). Ab initio calculations have been carried out on the IBM RS/6000 workstations by using the GAUSSIAN 94[36] program package.

REFERENCES

1. K. Yamaguchi, Y. Takahara and T. Fueno, in Applied Quantum Chemistry (V. H. Smith Jr, H. F. Schaefer III and K. Morokuma Eds., Reidel, 1986) p 155.
2. K. Yamaguchi and T. Fueno, Kagaku, 41, 372, 585 (1986) (In Japanese).
3. J. G. Bednort and K. A. Muller, Z. Phys., 64, 189 (1986).
4. (a) K. Yamaguchi, Y. Takahara, T. Fueno and K. Nasu, Jpn. J. Appl. Phys., 26, L1362 (1987); (b) Idem., ibid., 26, L2037 (1987); (c) Idem., Ibid., 27, L509, L766 (1988);
5. S. Yamamoto, K. Yamaguchi and K. Nasu, Phys. Rev., 42, 266 (1990).
6. K. Yamaguchi, Int. J. Quant. Chem., 37, 167 (1990).
7. K. Yamaguchi, the invited talk in the symposium on the specially promoted project "molecular magnetism" (1994, October, Tokyo).
8. (a) K. Yamaguchi, in a round Table talk in the NATO ASI meeting (Teneriffe, 1995, May); (b) D.Gatteschi and K. Yamaguchi, NATO ASI vol. p 567 (1996).

9. K. Yamaguchi, Kinouzairyou 7, 47 (1990) (In Japanese).
10. K. Yamaguchi, H. Namimoto, T. Fueno, T. Nogami and Y. Shirota, Chem. Phys.Lett., 166, 408 (1990).
11. (a) M. Okumura, W. Mori and K. Yamaguchi, in Comp. Aided Innov. of New Materials II (M. Doyama et al., Eds., Elsevier, Tokyo, 1993) p1785.(b) D. Yamaki, S. Yamada, G. Maruta, T. Kawakami, W. Mori and K. Yamaguchi, Mol. Cryst. Liq. Cryst., 279, 9 (1996); (c) G. Maruta, D. Yamaki, W. Mori, K. Yamaguchi and H. Nishide, ibid., 279, 19 (1996).
12. (a) M. Fujiwara, T. Matsushita, K. Yamaguchi and T. Fueno, Synthetic Metals 41-43, 3267 (1991); (b) M. Fujiwara, S. Takamizawa, W. Mori and K. Yamaguchi, Mol. Cryst. Liq. Cryst., 279, 1 (1996).
13. E. Coronado et al. Eds. NATO ASI series (1996).
14. W. R. Entley and G. S. Girolami, Inorg. Chem., 33, 5165 (1994).
15. W. R. Entley and G. S. Girolami, Science, 268, 397 (1995).
16. W. R. Entley, C. R. Treadway and G. S. Girolami, Mol. Cryst. Liq. Cryst., 273, 153 (1995).
17. T. Mallah, M. Thiebaut, M. Verdaguer and P. Veillet, Science, 262, 1554 (1993).
18. S. Ferlay, T. Mallah, R. Quahes, P. Veillet and M. Verdaguer, Nature, 378, 701 (1995).
19. V. Gadet, T. Mallah, I. Castro, M. Verdaguer and P. Veillet, J. Am. Chem. Soc., 114, 9213 (1992).
20. R. Klenze, B. Kanellakopulos, G. Trageser and H. H. Eysel, J. Chem. Phys., 75, 5819 (1980).
21. V. Gadet et al., D. Gatteschi et al., Eds., in Magnetic Molecular Materials, NATO ASI Series E., vol. 198, p281 (Plenum, New York, 1991).
22. O. Sato, I. Iyoda, A. Fujishima and K. Hashimoto, Science, 271, 49 (1996).
23. O. Sato, I. Iyoda, A. Fujishima and K. Hashimoto, Science, (1996) in press.
24. Z. Gu, O. Sato, I. Iyoda, K. Hashimoto and A. Fujishima, to be published.
25. (a)J. B. Goodenough, J. Phys. Chem. Solids, 6, 287 (1959); (b) J. Kanamori, ibid., 10, 87 (1959).
26. K. Yamaguchi, Y. Yoshioka and T. Fueno, Chem. Phys., 20, 171 (1977).
27. K. Yamaguchi, T. Tsunekawa, Y. Toyoda and T. Fueno, Chem. Phys. Lett., 143, 371 (1988)
28. K. Yamaguchi, T. Fueno, M. Ozaki, N. Ueyama and A. Nakamura, Chem. Phys. Lett., 168, 56 (1990).
29. C. Zener, Phys. Rev., 82, 403 (1951).
30. P. de Gennes, Phys. Rev., 118, 141 (1960).
31. H. Tatewaki and S. Hujinaga, J. Chem. Phys., 72, 339 (1980).
32. J. Hubbard, Proc. Roy. Soc. (London) A276, 238 (1963).
33. (a) K. Yamaguchi, M. Nakano, H. Namimoto and T. Fueno, Jpn. J. Appl. Phys., 27, L1835 (1988); (b)idem., ibid., 28, L479 (1989).
34. (a) S. Yamanaka, T. Kawakami, M. Okumura and K. Yamaguchi, Chem. Phys. Lett., 233, 257 (1995); (b) S. Yamanaka, M. Okumura, H. Nagao and K.Yamaguchi, ibid. 233, 88 (1995).
35. T. Sugawara, T. Sugimoto, T. Nogami, K. Nakasuji, private communications.
36. M. J. Frisch, G. W.Trucks, H. B. Schlegel, P. M. W. Gill, B. G. Johnson, M. A. Robb, J. R. Cheeseman, T. A. Keith, G. A. Petersson, J. A. Montgomery, K. Raghavachari, M. A. Al-Laham, V. G. Zakrzewski, J. V. Oritiz, J. B. Foresman, J. Cioslowski, B. B. Stefanov, A. Nanayakkara, M. Challacombe, C. Y. Peng, P. Y. Ayala, W. Chen, M. W. Wong, J. L. Andres, E. S. Replogle, R. Gomperts, R. L. Martin, D. J. Fox, J. S. Binkley, D. J. Defrees, J. Baker, J. P. Stewart, M. Head-Gordon, C. Gonzalez, and J. A. Pople, Gaussian, Inc., Pittsburgh PA, 1995.